

Hydrogeochemical study of spas groundwaters from southeast Brazil



Daniel Marcos Bonotto

Departamento de Petrologia e Metalogenia, Universidade Estadual Paulista (UNESP), Câmpus de Rio Claro, Av. 24-A No.1515, C.P. 178, CEP 13506-900 Rio Claro, São Paulo, Brazil

ARTICLE INFO

Article history:

Received 10 August 2015

Revised 17 March 2016

Accepted 17 July 2016

Available online 18 July 2016

Keywords:

Mineral waters

Spring waters

Hydrochemistry

Water classification

Southeast Brazil

ABSTRACT

This paper describes a hydrochemical study focusing spas groundwaters occurring at São Paulo and Minas Gerais states, Brazil, that are extensively used for drinking in public places, bottling and bathing purposes, among other. The water samples (75) for this study were taken from springs and pumped tubular wells drilled at different aquifer systems that are inserted in Paraná and Southeastern Shield hydrogeological provinces. The data acquisition for temperature, electrical conductivity (EC), pH, redox potential (Eh), dissolved gases (O₂, CO₂ and H₂S) and alkalinity was in situ performed for avoiding losses and modification due to transportation. The total dissolved solids (TDS) concentration was evaluated by gravimetry, the major cations and anions, iron and silica by colorimetry/atomic absorption spectrophotometry (AAS), and fluoride by potentiometry. The acquired database allowed establish the principal trends among the parameters analyzed after assuring its consistence from expected relationships found in hydrogeochemical surveys. The groundwaters are reducing (from pH and Eh data), there is a direct TDS-EC relationship, implying on a significant correlation between their ionic strength (IS) and EC. The major ions justifying such trends were sodium, (bi)carbonate, chloride, sulfate and phosphate that also correlated positively with the IS. The spas groundwaters were classified according to the guidelines of the Brazilian Code of Mineral Waters (BCMw) and EU directive for mineral waters. The major hydrochemical facies were also determined, as well the main sources influencing the groundwater composition and possible sub-surface temperatures.

© 2016 Published by Elsevier B.V.

1. Introduction

In the last few decades, the consumption of natural drinking water, either spring or mineral (bottled or not), increased in several countries. Despite drinking water has been used mostly as the tap water accessible in every household, many people believe that the naturally occurring waters are healthy and/or can be utilized for health cures, thus, exhibiting better quality than the tap water. Additionally, economic reasons have also favored their use as bottled waters so that the commercialization of mineral waters has widely increased, inclusive in Brazil where circa 20 million consumers are involved (SEBRAE, 2012).

The thermal and mineral waters use in Brazil is not recent due to arrival of European immigrants, mainly from Portugal. The construction of thermal and non-thermal spas for therapeutic and leisure purposes reached a maximum number in the 1930s and 1950s, mainly at São Paulo (SP) and Minas Gerais (MG) states (Mourão, 1992). The Brazilian Code of Mineral Waters (BCMw) was established in this time, under French influence, by Register 7841 published on 8 August 1945 (DFPM, 1966). It classifies the mineral waters for spas and bottling uses, as well the potable waters for bottling, including several

parameters like the radioactivity due to dissolved ²²²Rn and ²²⁰Rn (DFPM, 1966; Serra, 2009).

Some hydrogeochemical studies of Brazilian natural mineral waters took into account the BCMw guidelines. For instance, Bertolo et al. (2007) analyzed 303 labels of bottled mineral waters, grouping them according to the total dissolved solids (TDS) concentration. Oliveira et al. (2001) and Godoy et al. (2001) measured ²²⁶Ra, ²²⁸Ra and ²¹⁰Pb in 17 and 28 brands of bottled mineral waters, respectively. Szikszay (1981) realized a detailed hydrogeochemical survey at Águas da Prata (SP) spa, whereas Oliveira et al. (1998) evaluated the ²²²Rn e ²²⁶Ra seasonal variation there.

EuroGeoSurveys (The Geochemistry Group of the European Geological Surveys) managed a common European sampling campaign of bottled mineral and spring waters (analysis of 884 samples for >70 chemical parameters in one laboratory) whose results were published in 2010 in the Special Issue “Mineral Waters of Europe” of Journal of Geochemical Exploration (v. 107, pp. 217–422). The hydrogeochemical study held within the framework of the project involved different approaches like analytical techniques, major constituents, trace elements, radionuclides, stable isotopes, mapping, waters classification, statistical treatment of hydrochemical data, human health, etc. Water sources were from Croatia (Peh et al., 2010), Estonia (Bitjukova and Petersell, 2010), Germany (Birke et al., 2010a, 2010b), Greece (Demetriades, 2010; Dotsika et al., 2010), Hungary (Fugedi et al., 2010), Italy (Dinelli

E-mail address: danielmarcosbonotto@gmail.com.

et al., 2010; Cicchella et al., 2010), Norway/Sweden/Finland/Iceland (Frengstad et al., 2010), Portugal (Lourenço et al., 2010), Serbia (Petrović et al., 2010), Slovakia (Dušan et al., 2010), and Slovenia (Brenčič and Vreča, 2010; Brenčič et al., 2010).

DNPM-National Department of Mineral Production manages in Brazil the production and commercialization of mineral waters. The amount of bottled mineral waters at SP in 2007 was higher than 1.5 billion liters (34% of the total in the country) (CPRM, 2012). The actual accentuated consumption of spring and mineral waters for drinking purposes in Brazil requests a better understanding of their composition as the available information is sparse without considering the various lithologies involved and the adoption of standardized procedures for sampling and analyses. They are widely exploited from spas located at SP and MG due to historical reasons and the generation of a consistent database from the use of the same experimental steps allowed new hydrogeochemical insights and a comparison with other water sources occurring elsewhere.

2. Study area

The groundwater samples (75) were taken from springs and pumped tubular wells from 14 spas located in SP and MG (Fig. 1) at various geological contexts: Águas de São Pedro (3), Águas da Prata (7), Águas de Lindóia (7), Serra Negra (8), Lindóia (2), Termas de Ibirá (5), Águas de Santa Bárbara (1), Lambari (6), São Lourenço (8), Cambuquira (6), Caxambu (10), Poços de Caldas (6), Pocinhos do Rio Verde (4) and Araxá (2). The water sources were from different aquifer systems in the Paraná and Southeastern Shield hydrogeological provinces (Table 1).

The spas of Águas de São Pedro, Águas de Santa Bárbara and Termas de Ibirá are in the Paraná basin, a huge sedimentary area of southern Brazil, with extensions into Paraguay, Uruguay and Argentina. The stratigraphical record of this intracratonic basin shows a tendency towards continental depositional systems (Milani, 2004). In the Neo-Ordovician, marine strata deposited from the onset of sedimentation continued throughout the Devonian with oceanic influence up to the Carboniferous (Milani,

2004). From Permian times on, the basin took the form of a large inland sea (Milani, 2004). Eolian sandstone beds came to dominate the Mesozoic scenario and with the break-up of Gondwana, the basin basement was much affected by the intrusion of vast amounts of magma emplaced as dykes and sills between the sedimentary strata as well as flows on the surface (Milani, 2004). The evolutionary history of the Paraná basin closed in the Early-Cretaceous with the deposition of continental sediments over the Serra Geral lavas (Milani, 2004). Different magma eruption rates ($\sim 0.1 \text{ km}^3 \text{ yr}^{-1}$ or $\geq 2.0 \text{ km}^3 \text{ yr}^{-1}$) and duration (11 Ma, from 140 Ma to 129 Ma; $< 1 \text{ Ma}$, began at 134.7 Ma) of the Paraná continental flood basalt (CFB) volcanism have been suggested from $^{40}\text{Ar}/^{39}\text{Ar}$ geochronology data (Renne et al., 1992; Turner et al., 1994; Thiede and Vasconcelos, 2010; etc.). The main rocks in the Paraná basin are sandstones, conglomerates, diamictites, tillites, siltstones, shales, rythmites, silex, mudstones, limestones, basalts and diabases (IPT, 1981). Deep tube wells have exploited groundwaters of the sampling points at Águas de Santa Bárbara spa (Serra Geral and Botucatu formations) and Águas de São Pedro spa (Tubarão Group) (Kimmelmann et al., 1987).

The spas of Águas de Lindóia, Serra Negra and Lindóia are in a region where various phases/cycles involving metamorphic, deformation and magmatic events have acted from the Archean to the Upper Proterozoic times. They have affected rocks of high metamorphic degree, generally of granulite and amphibolite facies (Ebert, 1955; Almeida and Hasui, 1984). The principal rocks occurring there are immature sediments (comprising sand, silt, clays and organic matter), milonites, quartzites, schists, gneisses, anfibolites, migmatites and syntectonic granites (Zanardo, 1987). The groundwater samples at Águas de Lindóia spa provided from fractures/fissures/faults occurring in migmatite (Lindália and Santa Isabel springs), quartzite (Comexim, Curie, Filomena and Beleza springs) and milonite/quartzite (São Roque spring) (del Rey, 1989).

The extensive Early-Cretaceous Paraná CFB province and a number of Early-Cretaceous to Eocene alkaline igneous provinces that surround the Paraná Basin like the Poços de Caldas alkaline massif (PCAM), Alto Paranaíba igneous province (APIP) and minor occurrences have been associated with the thermal and/or chemical influence of mantle-plumes (Tristan and Trindade) impacting on the base of the continental lithosphere (e.g. Gibson et al., 1995a, 1995b; Thompson et al., 1998).

The spas of Águas da Prata, Poços de Caldas and Pocinhos do Rio Verde are located in PCAM that is roughly circular (diameter $\sim 33 \text{ km}$) and covers $\sim 800 \text{ km}^2$. It is a suite of alkaline volcanic and plutonic rocks (mainly phonolites and nepheline syenites) whose evolutionary history starts with major early volcanism involving ankaratrites (biotite-bearing nepheline), phonolite lavas, and volcano-clastics, followed by caldera subsidence and nepheline syenite intrusions forming minor ring dykes and circular structures and, finally, the intrusion of eudialite-bearing nepheline syenites (Ellert, 1959; Schorscher and Shea, 1992; Ulbrich et al., 2005). The following springs were sampled at Águas da Prata spa: Villela and Boi (discharges into sandstones); Vitória and Prata (discharges through fissures in diabase); Platina, Paiol and Padre (discharges through volcanic tuffs, phonolites and eudialite-bearing nepheline syenites) (Szikszay, 1981). Groundwaters at Poços de Caldas and Pocinhos do Rio Verde spas were from thermal/non-thermal springs discharging in crystalline fractured rocks (Cruz and Peixoto, 1989).

Araxá spa is located at APIP, including the renowned Araxá carbonatite circular intrusion (diameter $\sim 4.5 \text{ km}$) (Traversa et al., 2001). The APIP is one of the world's most voluminous mafic potassic provinces composed of a relatively diverse suite of ultrapotassic-potassic, ultramafic-mafic, silica-undersaturated lavas and hypabyssal intrusions with very high concentrations of incompatible trace elements and strongly enriched in light rare earths relative to heavy rare earth elements (Gibson et al., 1995b; Gomes and Comin-Chiaramonti, 2005). A



Fig. 1. Sketch map of the research region in Brazil and location of the groundwater sampling points in the following spas of São Paulo and Minas Gerais states: ASP = Águas de São Pedro, ADL = Águas de Lindóia, SEN = Serra Negra, LIN = Lindóia, TEI = Termas de Ibirá, ASB = Águas de Santa Bárbara, ADP = Águas da Prata, PDC = Poços de Caldas, PRV = Pocinhos do Rio Verde, LAM = Lambari, SLO = São Lourenço, CAM = Cambuquira, CAX = Caxambu, AXA = Araxá.

Table 1
Description of the water samples analyzed in this paper.

City (State ^a)	Spring (well) name/sample code	Hydrogeological province ^b	Dominant flow	Major rock types	Geological context/age	Commercialization ^c
Águas de São Pedro (SP)	Almeida Salles/ALS Gioconda/GIO Juventude/JUV	Paraná	Porous	Sandstones	Botucatu Fm. (Jurassic) Pirambóia Fm. (Triassic) Itararé Fm. (Permian) Irati Fm. (Permian)	
Águas da Prata (SP)	Platina/PLA Paiol/POL	Paraná	Fractures	Diabases Phonolites	Botucatu Fm. (Jurassic) Serra Geral Fm. (Jurassic–Cretaceous)	Yes
	Vitória/VIT Boi/BOI Prata/PTA Vilela/VIL Padre/PDE			Alkaline rocks Silicified sandstones	Poços de Caldas intrusive complex (Cretaceous)	Yes
Águas de Lindóia (SP)	Santa Isabel/SIL Filomena/FIL Beleza/BEL São Roque/SRE Comexim/COM Lindália/LIN Curie/CUR	Paraná	Fractures	Granites Gneisses Migmatites Schists Quartzites Limestones Dolomites	Amparo Gp. (Lower Proterozoic)	Yes Yes
Serra Negra (SP)	São Jorge/SJO São Carlos/SCA Italianos/ITA Santa Luzia/SLU Santo Agostinho/SAT Brunhara/BRU Laudo Natel/LAN Sant'Anna/SAA					
Lindóia (SP)	São Benedito/SBE Bioleve/BIO					Yes Yes
Termas de Ibirá (SP)	Jorrante/JOR	Paraná	Porous and fractures	Sandstones Basalts	Bauru Gp. (Cretaceous) Serra Geral Fm. (Jurassic–Cretaceous)	
	Ademar de Barros/ADB Carlos Gomes/CGO Saracura/SRC Seixas/SEI					
Águas de Santa Bárbara (SP)	Balneário Municipal/BMU	Paraná	Porous and fractures	Sandstones Basalts	Bauru Gp. (Cretaceous) Serra Geral Fm. (Jurassic–Cretaceous)	
Lambari (MG)	No. 1/LA1 No. 2/LA2 No. 3/LA3 No. 4/LA4 No. 5/LA5	Southeastern shield	Porous and fractures	Ortogneisses Granulites Migmatites Metasedimentary seq. Metavulcanosedimentary seq.	Paraíba do Sul Gp. (Proterozoic) Barbacena Gp. (Proterozoic) São João d'el Rei Gp. (Proterozoic) Andrelândia Gp. (Proterozoic) Magmatic plutonic series (Brasiliano)	
São Lourenço (MG)	No. 6/LA6 No. 7-Bis/SL7 No. 5-Alcalina/SL5 No. 6-Sulfurosa/SL6 No. 3-Vichy/SL3 No. 4-Ferruginosa/SL4 No. 1-Oriente/SL1 No. 10-Primavera/SL10 No. 9-Carbogosa/SL9					
Camuquira (MG)	Roxo Rodrigues/ROR Regina Werneck/REW Com. Augusto Ferreira/CAF Fernandes Pinheiro/FEP Marimbeiro/MAR Souza Lima/SLI					
Caxambu (MG)	Geiser Floriano de Lemos/GFL Venâncio/VEN Mayrink/MAY Ernestina Guedes/EGU Viotti/VIO D. Pedro II/DPE Beleza/BZA Duque de Saxe/DXE Da. Leopoldina/LEO Da. Isabel/Conde d'Eu/ISA					

Table 1 (continued)

City (State ^a)	Spring (well) name/sample code	Hydrogeological province ^b	Dominant flow	Major rock types	Geological context/age	Commercialization ^c
Poços de Caldas (MG)	Quisiana/QUI XV de Novembro/NOV Macacos/MAC Sinhazinha/SIN Frayha/FRA Pedro Botelho/PEB	Southeastern shield	Fractures	Alkaline rocks Nepheline syenites Phonolites Pyroclastics Volcanic tuffs	Poços de Caldas intrusive complex (Cretaceous)	
Pocinhos do Rio Verde (MG)	Rio Verde/RIV Samaritana/SMA São José/SJO Amorosa/AMO					
Araxá (MG)	Dona Beja/DBJ Andrade Júnior/AJU	Southeastern shield	Porous and fractures	Quartzites and schists Alkaline-carbonatitic rocks	Cretaceous PreCambrian	

^a SP = São Paulo State, MG = Minas Gerais State.

^b According to [Mente \(2008\)](#).

^c Water commercialized by private company in addition to consumption in taps accessible to population in public areas.

complex network of carbonatite as concentric and radial dykes quite variable in dimension and also small veins ranging from few millimeters to several centimeters in thickness are present in the region of Araxá spa, intruding either alkaline or country rocks. Additional lithologies include mica-rich rocks, phoscorites and lamprophyres ([Traversa et al., 2001](#)). Two springs were sampled at Araxá spa: 1) Dona Beja, associated to an aquifer system classified as granular, free and semi-confined, mainly in the intrusive body domain ([Beato et al., 2000](#)); 2) Andrade Júnior, related to a deep fractured aquifer, unconfined to semi-confined, mainly occurring in rocks surrounding the carbonatite complex ([Beato et al., 2000](#)).

Minor alkaline occurrences representing multi-stage intrusions emplaced into Late-Proterozoic metamorphic rocks were reported by [CPRM \(1999, 2008\)](#) during mapping of south MG where are located Lambari, São Lourenço, Cambuquira and Caxambu spas. The main rocks in the region are biotite gneisses, migmatized granitoids, protomylonites, mylonite gneisses, metabasites intercalations secondarily cut by pegmatoids veins, schists, weathered quartzites and alluvial deposits. The gneissic rocks in Caxambu hill are cut by mafic dykes and alkaline breccias, constituting important recharge areas of the fractured aquifers ([CPRM, 1999](#)). In São Lourenço, Lambari and Caxambu spas, the rainwater infiltration in weathered horizons of gneissic rocks is followed by percolation through mylonitized zones and fractures partially filled by pegmatoids dykes/alkaline breccias ([CPRM, 1999](#)). The periodical eruption of a non-geothermal geyser (~5-m high) occurs at Caxambu spa due to the pressure build-up from dissolved CO₂ in water.

3. Experimental

One groundwater sample from each point was collected during the dry season (June–September) for avoiding contribution of recent recharged rainwater. This limited number of samples was due to the size of the study area and costs involved for field trips and analyses. With exception of geyser “Floriano de Lemos” (code GFL), all water sources have been used for drinking purposes, whilst some have been commercialized by private companies under different brands ([Table 1](#)).

The data acquisition for temperature, electrical conductivity (EC), pH, redox potential Eh, dissolved gases (O₂, CO₂ and H₂S) and alkalinity happened in situ for avoiding losses/modification due to transportation. The groundwater samples (~3 L) were collected from taps/pipes installed in each spring/well, stored in polyethylene bottles and transported to LABIDRO-Isotopes and Hydrochemistry Laboratory, Rio Claro city, for chemical analysis. Each sample was divided into different aliquots and unfiltered + unpreserved or filtered through 0.45 μm

Millipore membrane + preserved with different acids, depending on the requirements of the analyses.

Digital meters were used for recording the following parameters: temperature - through a thermocouple sensor; pH - through a combination glass electrode and buffer solutions for calibration; Eh - through a combination Pt electrode-Ag/AgCl reference element and a Zobell I ([Zobell, 1946](#)) standard solution; EC - through a 1 cm² area Pt electrode calibrated with KCl standards; dissolved oxygen (DO) concentration - through a O₂ sensible electrode, i.e. a metallic wire covered by a thin Au layer; fluoride - through an ion-selective electrode and standards with variable F⁻ concentrations. The Eh readings were done adopting the procedure described by [Bonotto \(2006\)](#), whereas all DO data were properly corrected due to altitude differences of the sampling points ([Hach, 1992](#)).

The total alkalinity (ALK) was determined by titration to an end-point evidenced by the color change of a standard indicator solution of the bicarbonate, carbonate and hydroxide concentrations ([APHA, 1989; Hach, 1992](#)). Titration with phenolphthalein indicator + 0.0227 N NaOH solution was adopted to evaluate the dissolved CO₂ (in mg/L) from the titrant volume used (in mL) ([Hach, 1992](#)). The dissolved CO₂ corresponded to 0 mg/L when the color changed after the indicator addition, without the need of adding titrant ([Hach, 1992](#)).

The dissolved sulfide gas (in mg/L sulfide, S²⁻) was determined by colorimetry (wavelength 665 nm) using a program stored in the Hach DR/2000 spectrophotometer ([Hach, 1992](#)). The methylene blue method was adopted in which the H₂S and acid-soluble metal sulfides reacted with *N,N*-dimethyl-*p*-phenylenediamine oxalate to form methylene blue ([Hach, 1992](#)). The intensity of the blue color was proportional to the S²⁻ concentration, whilst dilutions were used to determine high levels in some samples.

The dry residue (DR) (~TDS, total dissolved solids) content was evaluated by evaporation and weighing ([APHA, 1989](#)). Atomic absorption spectrophotometry (AAS) was used to measure the dissolved Na⁺ concentration, whereas colorimetry for characterizing the dissolved K⁺, Ca²⁺, Mg²⁺, Cl⁻, NO₃⁻, SO₄²⁻, PO₄³⁻, Fe, Fe²⁺ and SiO₂ concentrations. Various reagents added to the samples produced colored complexes read by a program stored in Hach DR/2000 spectrophotometer that had been previously calibrated ([Hach, 1992](#)). [Table 2](#) summarizes the methods adopted and respective detection limits.

4. Results

[Tables 3 and 4](#) report all data obtained. Aquachem 4.0 software ([Waterloo Hydrogeologic, 2003](#)) evaluated the ionic strength (IS) of the waters ([Table 3](#)) and performed the statistical data treatment ([Table 5](#)).

Table 2
Analytical methods and detection limits.

Parameter	Unit	Analytical method	Detection limit	Parameter	Unit	Analytical method	Detection limit
Temp.	°C	Potentiometric	–	Na	µg/L	AAS	0.3
pH	–	Potentiometric	–	K	mg/L	Colorimetric	0.13
Eh	mV	Potentiometric	–	Ca	µg/L	Colorimetric	20
EC	µS/cm	Conductometric	–	Mg	µg/L	Colorimetric	6
DO	mg/L	Potentiometric	0.1	SiO ₂	mg/L	Colorimetric	0.45
CO ₂	mg/L	Titration	–	Cl [–]	mg/L	Colorimetric	0.3
H ₂ S	µg/L	Colorimetric	1	F [–]	µg/L	Potentiometric	20
TDS	mg/L	Gravimetric	1	NO ₃ [–]	mg/L	Colorimetric	0.8
ALK	mg/L	Titration	1	SO ₄ ^{2–}	mg/L	Colorimetric	0.5
Fe _{tot}	µg/L	Colorimetric	6	PO ₄ ^{3–}	µg/L	Colorimetric	20
Fe ²⁺	µg/L	Colorimetric	6				

EC = electrical conductivity; DO = dissolved oxygen; TDS = total dissolved solids; ALK = total alkalinity; AAS = atomic absorption spectroscopy.

Table 3
Physicochemical data of the waters analyzed in this study.

Sample code	Temp. (°C)	Eh (mV)	EC (µS/cm)	DO (mg/L)	CO ₂ (mg/L)	H ₂ S (µg/L)	ALK (mg/L)	SiO ₂ (mg/L)	Fe _{tot} (mg/L)	Fe ²⁺ (mg/L)	TDS (mg/L)	IS (×10 ^{–4})	
ALS	27.1	7.40	16	710	3.13	120	3	261	39.7	0.03	b.d.	1880	30.8
GIO	27.4	8.45	–59	3790	5.08	100	6	204	12.8	0.01	b.d.	1700	167.7
JUV	26.7	8.59	–59	4730	2.81	88	3064	338	24.5	0.66	b.d.	1960	189.5
PLA	25.4	8.21	–5	1530	1.33	400	5	472	33.1	0.01	b.d.	936	101.0
POL	25.8	8.23	–37	3630	3.06	800	12	1390	29.0	0.02	b.d.	2625	260.8
VIT	24.5	9.23	–150	3370	1.33	1032	2	1388	32.8	0.06	b.d.	1042	311.3
BOI	24.2	7.57	–154	40	3.77	128	4	17	18.6	0.22	0.01	54	9.8
PTA	25.1	7.17	–25	280	7.14	180	4	73	19.7	0.01	b.d.	2215	11.4
VIL	24.3	7.98	–159	30	5.71	140	3	2	8.9	0.05	b.d.	43	4.9
PDE	23.7	6.74	–52	220	5.10	256	4	99	19.3	b.d.	b.d.	240	13.5
SIL	22.5	6.94	–27	160	5.35	96	1	36	17.0	b.d.	b.d.	59	6.2
FIL	26.9	7.86	–33	220	4.65	108	2	65	14.1	0.05	b.d.	38	8.8
BEL	26.4	7.89	–17	210	3.84	88	2	69	17.3	0.11	b.d.	89	8.3
SRE	27.3	7.52	6	230	4.44	164	2	58	15.7	0.02	b.d.	74	7.3
COM	23.6	5.61	97	20	6.06	100	1	11	12.3	0.15	b.d.	11	3.1
LIN	24.6	6.98	–3	360	5.66	136	4	76	37.5	0.02	0.02	86	17.4
CUR	26.2	6.86	–38	180	4.65	128	5	60	17.6	0.01	b.d.	154	8.8
SJO	22.0	5.92	–54	140	6.16	132	2	16	18.5	b.d.	b.d.	172	7.6
SCA	21.7	5.85	7	220	5.66	236	b.d.	71	34.3	0.01	b.d.	233	11.2
ITA	20.4	6.18	–38	210	5.66	212	8	62	34.1	b.d.	b.d.	193	10.4
SLU	21.5	5.94	–25	130	2.83	188	1	35	25.3	0.02	b.d.	225	8.0
SAT	21.8	5.87	–30	170	3.23	236	2	43	28.8	b.d.	b.d.	167	9.3
BRU	22.1	5.94	–28	180	4.85	160	1	27	32.5	b.d.	b.d.	144	9.0
LAN	23.1	5.62	–1	130	3.64	212	3	21	20.1	b.d.	b.d.	106	8.3
SAA	21.9	6.07	–55	150	4.65	200	1	52	35.0	b.d.	b.d.	185	9.6
SBE	24.9	6.47	–50	290	9.05	180	3	83	40.6	0.12	b.d.	286	13.6
BIO	23.6	5.96	–74	90	6.45	132	3	24	20.3	0.14	b.d.	134	6.5
JOR	26.8	9.03	–144	660	2.05	0	13	99	34.3	0.01	b.d.	410	52.8
ADB	28.4	8.96	–145	670	2.59	0	3	130	32.4	0.01	b.d.	420	51.9
CGO	28.4	9.09	–147	680	1.30	0	5	98	34.6	0.05	b.d.	380	46.1
SRC	28.7	9.17	–150	700	0.97	0	35	90	33.4	b.d.	b.d.	460	41.9
SEI	26.4	8.97	–138	640	2.38	0	8	105	37.3	b.d.	b.d.	455	44.7
BMU	24.6	7.58	112	160	5.99	252	2	73	39.2	b.d.	b.d.	200	21.6
LA1	23.0	4.55	–90	190	5.00	1840	1	25	11.5	0.01	b.d.	121	8.3
LA2	23.0	4.53	–91	190	4.69	1600	2	19	12.7	0.04	0.01	212	7.9
LA3	23.1	4.90	–87	220	4.49	1480	1	28	11.7	0.02	0.01	198	8.9
LA4	24.0	4.16	32	190	4.69	600	b.d.	34	9.6	0.02	0.01	256	11.2
LA5	25.4	4.71	–50	170	6.73	1840	b.d.	22	17.0	1.14	0.01	446	7.4
LA6	24.0	4.81	–67	160	5.51	1480	b.d.	21	14.5	0.12	b.d.	139	6.5
SL7	24.7	6.17	–67	620	1.53	800	18	158	34.8	1.55	0.02	198	24.7
SL5	23.6	6.38	–56	1030	1.73	1560	b.d.	262	23.2	0.19	b.d.	185	37.8
SL6	25.2	6.18	–39	1180	1.22	1720	b.d.	292	41.0	5.18	0.03	323	42.6
SL3	26.7	6.59	–64	1050	3.67	1320	b.d.	303	38.7	1.10	b.d.	214	39.9
SL4	26.6	6.06	–65	660	1.94	920	b.d.	93	21.0	1.15	b.d.	305	20.8
SL1	25.6	5.97	–44	670	1.33	1420	b.d.	163	17.9	0.03	0.01	296	27.6
SL10	25.2	6.59	–58	1710	3.06	1200	b.d.	495	34.4	0.09	b.d.	176	66.9
SL9	23.9	5.94	–57	640	1.02	1480	b.d.	162	21.3	3.66	0.04	295	28.3
ROR	24.0	4.90	–37	90	3.74	800	1	2	18.6	0.05	0.01	126	4.4
REW	24.0	4.64	–23	90	3.03	1380	3	4	15.4	0.04	0.02	73	4.4
CAF	26.3	4.60	–38	100	4.34	1000	1	1	11.7	0.05	0.03	40	4.0
FEP	25.0	5.50	–35	240	2.63	1760	40	50	61.9	2.07	0.33	257	12.2
MAR	25.5	5.76	–42	570	3.33	1200	4	130	60.9	2.33	0.02	249	19.9
SLI	23.2	5.30	–24	170	3.13	1080	13	31	16.4	4.26	2.54	82	8.2
GFL	23.8	7.00	–39	2440	4.69	1100	14	919	44.2	1.11	0.99	1241	106.2
VEN	25.0	6.43	–51	2420	2.86	1680	17	784	38.9	0.27	0.23	757	92.1

Table 3 (continued)

Sample code	Temp. (°C)	pH	Eh (mV)	EC (µS/cm)	DO (mg/L)	CO ₂ (mg/L)	H ₂ S (µg/L)	ALK (mg/L)	SiO ₂ (mg/L)	Fe _{tot} (mg/L)	Fe ²⁺ (mg/L)	TDS (mg/L)	IS (×10 ⁻⁴)
MAY	25.5	5.29	-26	260	4.18	800	4	75	20.7	0.09	0.02	221	12.8
EGU	25.8	6.25	-68	2470	1.73	1600	b.d.	755	55.0	1.66	0.06	516	91.8
VIO	25.3	5.40	-59	400	1.84	800	15	130	23.4	0.03	b.d.	179	18.2
DPE	24.7	5.59	-66	620	1.94	880	9	153	21.7	0.03	b.d.	170	22.0
BZA	23.9	6.41	-65	3010	1.84	1440	1	680	60.2	3.18	2.94	757	94.3
DXE	25.4	6.23	-27	2040	1.84	720	7	643	42.3	0.11	0.09	820	76.0
LEO	24.5	5.97	-52	980	1.02	680	47	253	43.5	0.05	0.01	315	32.7
ISA	24.2	5.99	-74	2020	1.53	920	10	560	63.5	3.86	0.10	700	68.0
QUI	22.4	6.13	-41	170	2.25	104	1	10	9.9	0.04	b.d.	38	20.9
NOV	25.7	9.38	-53	920	1.37	0	259	196	28.4	0.04	b.d.	398	74.3
MAC	32.1	9.60	-51	1450	0.78	0	1184	233	31.0	0.01	b.d.	579	96.4
SIN	25.7	9.54	-90	1420	2.94	140	3	261	32.2	0.02	b.d.	574	114.1
FRA	23.2	6.91	-27	50	3.82	52	b.d.	6	6.7	0.14	b.d.	70	5.8
PEB	35.7	9.58	-70	1400	1.18	0	383	252	28.5	0.06	b.d.	600	117.2
RIV	23.3	9.10	-133	1290	1.30	180	756	270	30.5	0.02	b.d.	567	106.9
SMA	23.9	9.05	-133	1300	1.40	80	522	291	28.3	b.d.	b.d.	773	107.9
SJO	22.0	8.98	-133	1290	1.30	60	528	318	29.3	b.d.	b.d.	424	109.5
AMO	21.7	5.56	-18	40	5.80	112	4	5	11.0	b.d.	b.d.	48	3.2
DBJ	22.1	7.50	-146	330	5.00	252	1	112	23.4	0.06	b.d.	70	14.0
AJU	29.0	9.57	-141	6390	1.60	0	1980	2212	20.3	0.04	b.d.	2898	793.6

EC = electrical conductivity; DO = dissolved oxygen; ALK = total alkalinity; TDS = total dissolved solids; IS = ionic strength; b.d. = below detection limit.

The criterion generally adopted to check the reliability and completeness of the hydrogeochemical data is that the deviation of the neutral ion balance should be lower than 5% (Schoeller, 1962; Custodio and Llamas, 1976; Appelo and Postma, 2004). Aquachem 4.0 software (Waterloo Hydrogeologic, 2003) allowed find such values in only 4 water sources, possibly due to errors in the hydrogen carbonate determination, effects of waters containing very low to low mineral concentration and accentuated SiO₂ contribution in the hydrochemistry. Silica is high in all waters analyzed as shown in the Schoeller (1962) diagrams plotted in Figs. 2 and 3 according to the four TDS classes defined by the EU mineral waters directive (van der Aa, 2003). Despite SiO₂ is not taken into account on the “neutrality condition” evaluation (Schoeller, 1962; Custodio and Llamas, 1976; Appelo and Postma, 2004), the quartz solubility increases rapidly at pH > 9, causing the silicic acid (H₄SiO₄) deprotonation and forming the anion H₃SiO₄⁻. Ritter (2012) identified this process when used the PHREEQC software for calculating the concentration of dominant solutes in spring waters of Poços de Caldas (MG) spa.

High-fluoride groundwaters are a recognized feature of a number of aquifers across the world (Smedley et al., 2002; Reddy et al., 2010; Edmunds and Smedley, 2013; etc.). The F⁻/Cl⁻ molar ratios > 1 in several water sources from PCAM indicate that F⁻ is dominant relative to Cl⁻, whilst its importance is highlighted in the Piper (1944) diagram shown in Fig. 4. It also shows that bi(carbonate) and sodium ions dominate the water sources as confirmed by the following hydrochemical facies from the Aquachem 4.0 software (Waterloo Hydrogeologic, 2003): mixed (cations)-HCO₃⁻, Na⁺-mixed (anions), Na⁺-HCO₃⁻, Ca²⁺-HCO₃⁻, Na⁺-CO₃²⁻ and Na⁺-HCO₃⁻-CO₃²⁻. Additionally, other water types also occur like mixed (cations and anions), mixed (cations)-Cl⁻ and K⁺-mixed (anions).

4.1. Groundwater classification

The BCMW establishes different waters classification based on temperature and chemical aspects (DFPM, 1966). According to temperature, they are cold (25 °C, 41 water sources - 54.7%), hypothermal (25–33 °C, 33 water sources - 44%), and mesothermal (33–36 °C, 1 water source - 1.3%). Other classes defined by the BCMW are (DFPM, 1966): radiferous, radioactive, thoriferous, carbogaseous, bicarbonate-alkaline, earth-alkaline, sulfated, sulfured, nitrated, chlorinated and feruginous. Among these criteria, the BCMW guidelines for sulfur (dissolved sulfur > 1 mg/L) and iron (dissolved iron > 5 mg/L) suggest that the springs JUV (Águas de São Pedro-SP), MAC (Poços de Caldas-MG)

and AJU (Araxá-MG) are sulfured, whereas the spring SL6 (São Lourenço-MG) is ferruginous.

The BCMW differs of the EU mineral water directive adopted by various European countries during the evaluation of the EuroGeoSurveys database (van der Aa, 2003). It will be also used here and, from the TDS classes, the waters analyzed in this research exhibit very low mineral concentration (TDS < 50 mg/L – 6 samples, 8%), low mineral concentration (TDS 50–500 mg/L – 50 samples, 66.7%), intermediate mineral concentration (TDS 500–1500 mg/L – 13 samples, 17.3%), and high mineral concentration (TDS > 1500 mg/L – 6 samples, 8%).

Additionally, the EU directive (van der Aa, 2003) allows classify the water sources as: containing bicarbonate (HCO₃⁻ > 600 mg/L – 9.3%, sample codes POL, VIT, GFL, VEN, EGU, BZA and DXE), containing sulfate (SO₄²⁻ > 200 mg/L – 1.3%, sample code GIO), containing iron (Fe²⁺ > 1 mg/L – 4%, sample codes SLI, GFL and BZA), containing sodium (Na⁺ > 200 mg/L – 8%, sample codes GIO, JUV, PLA, POL, VIT and AJU), containing fluoride (F⁻ > 1 mg/L – 32%, 24 water sources), acid (CO₂ > 250 mg/L – 48%, 36 water sources), and suitable for low sodium diets (Na⁺ < 20 mg/L – 54.7%, 41 water sources). Therefore, most of the spas groundwaters are acid and suitable for low sodium diets, various contain fluoride and none exhibited chloride, calcium and magnesium concentrations above the EU reference values for mineral waters (Cl⁻ > 200 mg/L, Ca²⁺ > 150 mg/L and Mg²⁺ > 50 mg/L).

5. Discussion

5.1. Groundwater composition and human health

The Regulation on the Hygienic Acceptability of Potable Water given by the World Health Organization (WHO) defines the Maximum Acceptable Concentration of chemical substances in water for public water supply that corresponds to 1.5 mg/L for fluoride (WHO, 2011). Five water sources (codes DXE, SL4, SL6, SL7 and SL10) exhibited dissolved F⁻ concentration between 1 and 1.5 mg/L. They are suitable for human consumption (WHO, 2011) and mineral waters according to the EU directive (van der Aa, 2003). The WHO (2011) guideline reference value of 1.5 mg/L for fluoride has been exceeded in 19 water sources (25.3%) that are located at Águas de São Pedro (SP), Águas da Prata (SP), Poços de Caldas (MG), Pocinhos do Rio Verde (MG), São Lourenço (MG), Caxambu (MG), and Araxá (MG) spas. Such number is higher than 16% as reported by Eupedia (2016) for the analyses of different mineral water brands. It requires effective actions from the

Table 4

Chemical data of the waters analyzed in this study. All results in mg/L.

Sample code	Na ⁺	K ⁺	Ca ²⁺	Mg ²⁺	HCO ₃ ⁻	CO ₃ ²⁻	OH ⁻	Cl ⁻	F ⁻	NO ₃ ⁻	SO ₄ ²⁻	PO ₄ ³⁻
ALS	26.9	5.38	0.29	0.45	261	0	0	11.6	0.07	1.4	1	0.19
GIO	459.0	1.90	0.13	0.82	204	0	0	27.0	7.06	0.9	225	0.06
JUV	598.0	1.16	1.11	0.08	338	0	0	28.4	8.30	11.2	126	0.08
PLA	200.0	3.99	0.04	0.98	472	0	0	10.2	19.71	8.5	37	0.22
POL	532.0	9.84	0.02	1.00	1390	0	0	16.9	32.37	1.2	90	0.15
VIT	567.0	13.11	0.89	0.93	1134	254	0	23.5	18.36	6.6	111	0.09
BOI	1.9	8.28	0.06	0.74	17	0	0	24.5	0.26	1.3	11	0.05
PTA	5.3	4.58	0.06	0.64	73	0	0	5.9	0.41	1.4	8	0.40
VIL	0.6	3.44	0.62	0.24	2	0	0	2.9	0.08	7.8	2	0.04
PDE	5.0	5.35	3.12	0.44	99	0	0	3.0	0.50	1.5	3	0.17
SIL	3.1	2.56	0.09	0.90	36	0	0	3.2	0.12	2.3	1	0.10
FIL	2.3	3.20	0.84	0.75	65	0	0	2.2	0.12	2.6	1	0.07
BEL	1.9	2.24	0.07	0.62	69	0	0	2.3	0.11	2.2	1	0.13
SRE	1.8	4.36	0.03	0.60	58	0	0	2.9	0.12	1.2	1	0.29
COM	0.7	0.65	0.21	0.31	11	0	0	2.5	0.09	1.4	3	0.02
LIN	15.7	3.96	0.02	0.60	76	0	0	9.3	0.36	8.7	11	0.51
CUR	1.3	3.66	3.33	0.52	60	0	0	2.3	0.09	1.3	b.d.	0.11
SJO	4.8	1.03	3.36	0.68	16	0	0	8.8	0.10	4.0	1	0.13
SCA	5.7	2.96	3.06	0.35	71	0	0	3.8	0.11	3.4	b.d.	0.33
ITA	5.6	2.78	3.18	0.49	62	0	0	3.6	0.11	2.9	1	0.17
SLU	5.9	1.15	3.24	0.64	35	0	0	4.6	0.07	1.9	b.d.	0.11
SAT	5.9	1.33	3.30	0.60	43	0	0	7.8	0.10	2.4	b.d.	0.16
BRU	7.2	1.84	3.48	0.62	27	0	0	5.8	0.13	4.7	b.d.	0.25
LAN	5.6	0.94	3.45	0.66	21	0	0	8.3	0.07	4.4	b.d.	0.04
SAA	6.8	2.89	3.09	0.64	52	0	0	3.7	0.10	2.0	b.d.	0.22
SBE	8.2	3.72	3.00	0.43	83	0	0	7.8	0.10	3.9	1	0.15
BIO	2.6	4.40	3.09	0.59	24	0	0	2.6	0.07	2.0	b.d.	0.09
JOR	87.8	0.42	2.31	b.d.	0	82	17	7.8	0.44	1.5	78	0.12
ADB	87.4	0.36	2.46	0.01	0	106	24	7.0	0.40	2.6	52	0.16
CGO	91.4	0.39	2.67	0.01	0	52	46	7.9	0.43	1.7	67	0.27
SRC	91.8	0.33	2.49	0.01	0	22	68	7.7	0.48	1.2	74	0.22
SEI	83.5	0.29	2.40	0.01	0	58	47	7.0	0.49	2.9	63	0.06
BMU	7.3	3.07	25.50	0.90	72	1	0	b.d.	0.02	0.6	b.d.	b.d.
LA1	4.5	5.60	3.42	0.65	25	0	0	5.9	0.10	3.3	1.0	0.04
LA2	4.3	4.95	3.39	0.65	19	0	0	8.0	0.10	3.1	2.0	0.06
LA3	6.3	4.48	3.48	0.62	28	0	0	6.7	0.08	3.6	b.d.	0.05
LA4	6.1	2.75	3.42	0.68	34	0	0	16.2	0.07	3.6	b.d.	0.02
LA5	2.5	5.24	3.48	0.75	22	0	0	3.4	0.32	2.2	1	0.09
LA6	2.5	4.40	3.39	0.78	21	0	0	3.4	0.08	1.8	1	0.04
SL7	23.4	19.84	3.39	0.37	158	0	0	4.6	1.18	1.0	2	0.23
SL5	48.5	20.10	2.94	0.06	262	0	0	5.4	0.59	1.8	b.d.	0.10
SL6	54.3	18.05	3.18	0.30	292	0	0	6.1	1.17	0.4	1	0.16
SL3	46.2	11.50	3.45	0.25	303	0	0	3.7	1.75	0.6	1	0.09
SL4	25.5	19.96	3.69	0.36	93	0	0	12.8	1.24	0.8	b.d.	0.06
SL1	33.7	17.24	3.42	0.17	163	0	0	12.8	0.15	1.1	3	0.09
SL10	85.6	23.85	3.27	0.12	495	0	0	3.4	1.07	5.9	b.d.	0.27
SL9	35.2	17.52	3.48	0.39	162	0	0	8.0	0.89	b.d.	3	0.07
ROR	2.6	1.92	3.39	0.68	2	0	0	1.7	0.11	1.6	b.d.	0.05
REW	2.8	0.73	3.39	0.45	4	0	0	2.0	0.04	1.6	b.d.	0.09
CAF	2.3	0.90	3.30	0.58	1	0	0	2.0	0.08	1.2	b.d.	0.17
FEP	12.8	6.60	3.87	0.73	50	0	0	3.7	0.60	1.0	b.d.	0.26
MAR	14.9	13.05	3.33	0.50	130	0	0	2.5	0.53	0.8	4	0.25
SLI	2.9	1.92	3.27	0.70	31	0	0	1.9	0.22	1.5	1	0.05
GFL	92.3	21.10	3.42	0.17	919	0	0	7.1	2.02	12.3	2	0.37
VEN	85.6	20.85	4.50	0.06	784	0	0	9.7	1.71	6.4	2	0.15
MAY	6.8	12.06	3.42	0.64	75	0	0	3.2	0.23	1.8	1	0.11
EGU	86.2	21.35	4.50	0.35	755	0	0	4.6	2.25	12.5	b.d.	0.13
VIO	9.6	15.48	3.81	0.57	130	0	0	2.5	0.33	1.3	1	0.13
DPE	18.6	16.48	3.42	0.51	153	0	0	2.4	0.42	1.5	1	0.14
BZA	108.8	25.25	4.95	0.37	680	0	0	5.6	2.31	18.1	4	0.12
DXE	75.1	21.50	3.99	0.01	643	0	0	3.3	1.34	3.8	b.d.	0.08
LEO	35.3	5.75	3.57	0.22	253	0	0	6.5	0.42	1.1	b.d.	0.25
ISA	67.2	23.20	4.05	0.19	560	0	0	3.8	1.83	1.5	1	0.21
QUI	10.4	8.94	1.03	0.33	10	0	0	11.0	0.07	7.6	b.d.	0.06
NOV	112.9	6.88	0.61	0.02	70	126	0	4.6	13.57	11.1	41	0.08
MAC	183.0	10.36	0.51	0.03	0	150	83	6.0	22.24	3.3	76	0.14
SIN	180.0	9.58	0.69	0.03	31	230	0	5.8	23.00	1.0	73	0.09
FRA	1.2	0.74	0.47	0.05	6	0	0	2.3	0.08	11.3	b.d.	0.02
PEB	183.0	11.12	0.68	0.04	4	248	0	5.7	22.20	1.9	75	0.13
RIV	182.0	9.33	2.13	0.01	86	184	0	7.9	25.24	1.0	76	0.16
SMA	182.7	10.47	2.28	0.02	123	168	0	7.5	26.36	1.0	78	0.05
SJO	178.0	10.62	2.43	0.02	142	176	0	7.3	26.05	1.3	78	0.07
AMO	0.4	1.68	2.43	0.03	5	0	0	2.0	0.07	1.9	b.d.	0.11
DBJ	2.1	8.84	0.17	0.32	112	0	0	2.1	0.29	5.3	3	0.29
AJU	1510.0	14.91	0.42	0.11	52	2160	0	48.0	9.00	2.3	189	1.36

b.d. = below detection limit.

Table 5
Statistical parameters of the waters analyzed in this study.

Parameter	Unit	Minimum	Lower quartile	Median	Upper quartile	Maximum
Temp.	°C	20.4	23.4	24.6	25.8	35.7
pH	–	4.16	5.86	6.41	7.94	9.60
Eh	mV	–159	–72	–52	–28	112
EC	µS/cm	20	170	360	1235	6390
DO	mg/L	0.78	1.78	3.13	4.77	9.05
CO ₂	mg/L	0	110	236	1056	1840
H ₂ S	µg/L	<1	2	4	13	3064
ALK	mg/L	1	32	93	261	2212
TDS	mg/L	11	135	229	459	2898
IS	× 10 ^{–4}	3.1	8.5	19.9	67.5	793.6
SiO ₂	mg/L	6.7	17.8	28.3	34.5	63.5
Fe _{tot}	mg/L	<0.006	0.01	0.04	0.14	5.18
Na ⁺	mg/L	0.4	4.4	12.8	86.8	1510.0
K ⁺	mg/L	0.29	2.08	4.95	11.78	25.25
Ca ²⁺	mg/L	0.02	0.76	3.18	3.42	25.50
Mg ²⁺	mg/L	<0.006	1.00	0.12	0.45	0.64
Cl [–]	mg/L	<0.3	48.0	3.1	5.6	7.8
F [–]	mg/L	0.02	0.10	0.40	1.73	32.27
NO ₃ [–]	mg/L	<0.8	1.3	1.9	3.6	18.1
SO ₄ ^{2–}	mg/L	<0.5	1	1	24	225
PO ₄ ^{3–}	mg/L	<0.02	0.07	0.12	0.18	1.36

EC = electrical conductivity; DO = dissolved oxygen; TDS = total dissolved solids; ALK = total alkalinity; IS = ionic strength.

national health agencies as dental fluorosis may develop from successive exposures to high F[–] concentrations during the water ingestion. This disease is a developmental disturbance leading to dental enamel with lower mineral content and increased porosity (Alvarez et al., 2009; Edmunds and Smedley, 2013).

The high dissolved SiO₂ levels in the water sources analyzed may imply on the health treatment. Davenward et al. (2013) used Si-rich mineral waters as non-invasive methods to reduce the body burden of aluminum in individuals with Alzheimer's disease and a control group (their carers and partners). Davenward et al. (2013) reported that drinking Si-rich mineral water (~1 L each day for 12 weeks) facilitated the Al removal via the urine in both patient and control groups without any concomitant effect upon the urinary excretion of the essential metals (Fe and Cu). Davenward et al. (2013) utilized the Malaysian mineral water “Spritzer” (35 mg/L of Si) in their experiments, suggesting other brands on sale in Britain with high Si levels (“Volvic”-20 mg/L; “Fiji”-45 mg/L). The highest dissolved SiO₂ concentration was 63.5 mg/L (Si concentration ~30 mg/L, code ISA in Table 3), almost the same level used by Davenward et al. (2013). This spring name remembers the visit of Isabel Princess and her husband to Caxambu spa in 1868 for her health treatment (infertility due to a profound anemia). She was cured after 1-month treatment with those waters also Fe-enriched (3.86 mg/L, Table 3).

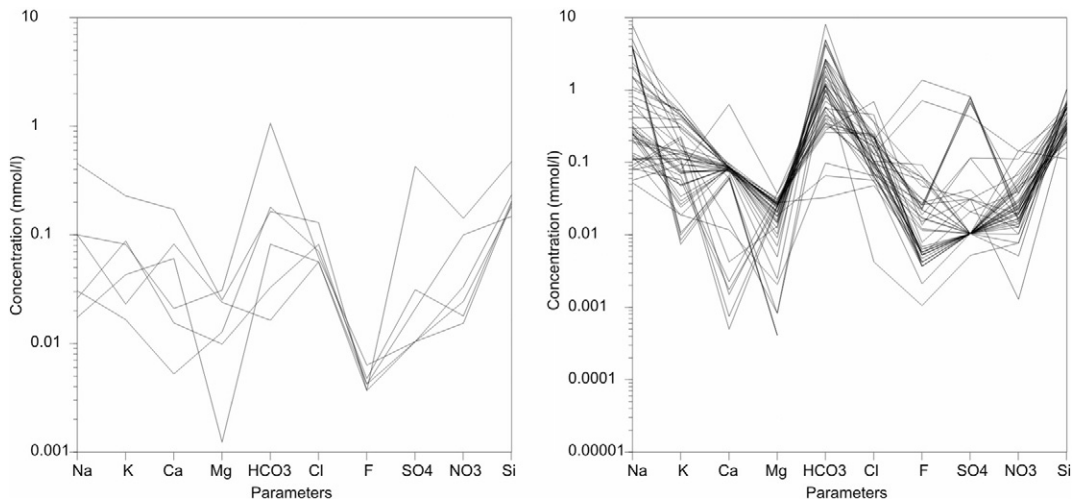


Fig. 2. Schoeller (1962) diagrams for the waters containing very low mineral concentration (TDS < 50 mg/L) (left) and low mineral concentration (TDS 50–500 mg/L) (right).

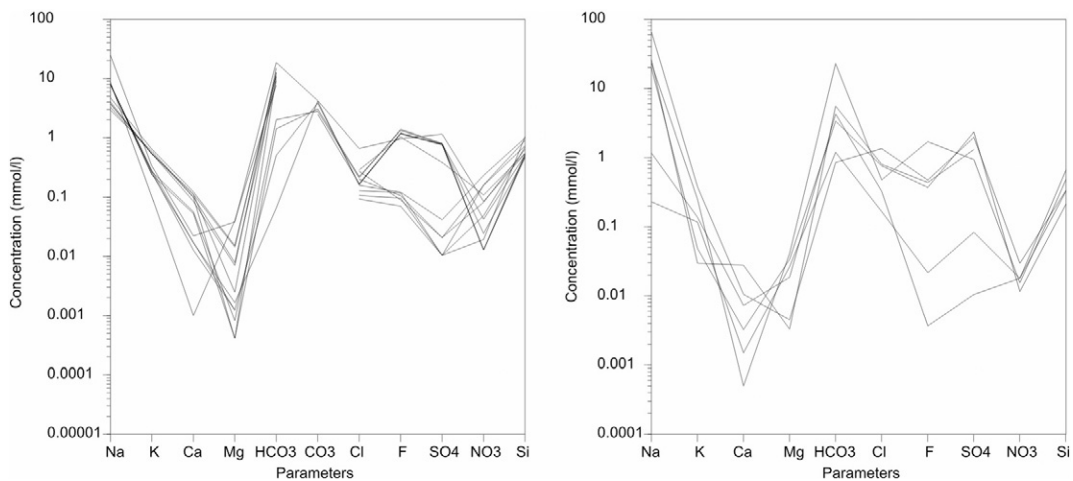


Fig. 3. Schoeller (1962) diagrams for the waters containing intermediate mineral concentration (TDS 500–1500 mg/L) (left) and high mineral concentration (TDS > 1500 mg/L) (right).

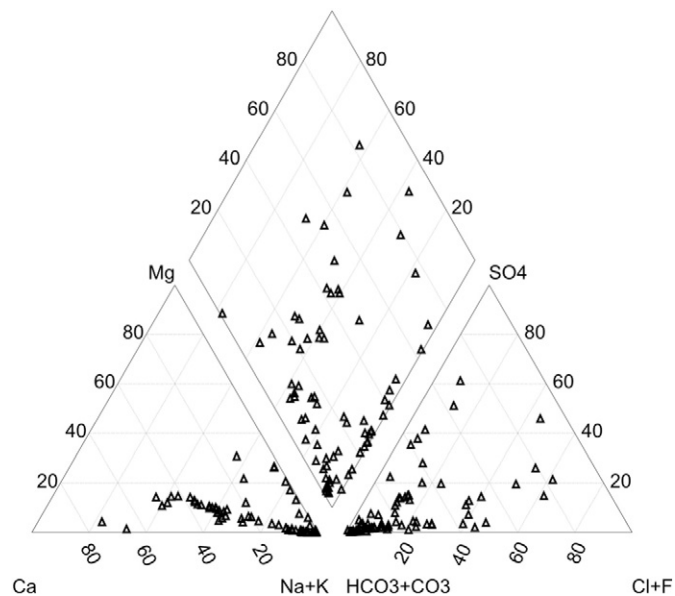


Fig. 4. Data of the groundwaters in this research plotted in a Piper (1944) diagram including the presence of the anion fluoride.

5.2. Major hydrochemical trends

The parameters pH and Eh reflect, respectively, the protons and electrons activities in the environment. The use of Eh-pH diagrams in geochemistry increased since the pioneering studies of Garrels (1959); Baas Becking et al. (1960) and Garrels and Christ (1965). Appropriate thermodynamic data have been utilized for many reactions occurring in temperature and pressure conditions different of those of the standard state (25 °C and 1 bar), despite the pressure changes do not introduce significant errors in the Eh-pH contours calculated at 1 bar

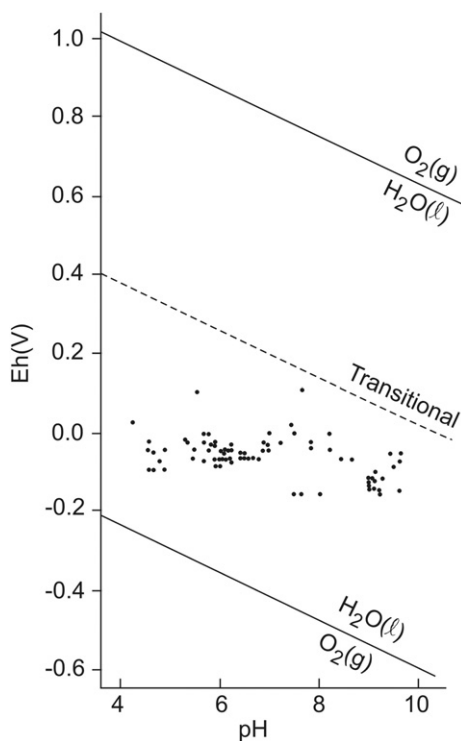


Fig. 5. Data of the groundwaters in this research plotted in an Eh-pH diagram as utilized by Krauskopf and Bird (1995).

(Brookins, 1988). In natural environments, oxidizing acid and reducing basic systems are often reported in the literature (e.g. Baas Becking et al., 1960; Krauskopf and Bird, 1995; Brownlow, 1996). The waters analyzed are reducing in character according to the Eh-pH diagram (Fig. 5).

The pH and Eh in the water sources may be controlled by the $\text{Fe}(\text{OH})_3\text{-Fe}_2\text{O}_3$ precipitation in the inert electrode as this is a common phenomenon in groundwater containing ferrous iron (Barnes and Back, 1964). Fig. 6 shows the pH and Eh data plotted in the activity diagram involving the chemical equilibrium between water and the system $\text{FeS-H}_2\text{S-H}_2\text{SO}_4$. Most of the samples are in the field of hematite coexisting with dissolved sulfate, whereas some are within the fields defined by pyrite and Fe^{2+} coexisting with dissolved sulfate, and pyrite coexisting with sulfur. The generation of sulfate from pyrite oxidation occurs in some sites according to the following reaction (Krauskopf and Bird, 1995):



However, the pH lowering associated to pyrite oxidation may not happen due to neutralization reactions involving the carbonates dissolution. Speciation calculations done with the Aquachem 4.0 software (Waterloo Hydrogeologic, 2003) yielded positive mineral saturation indices (oversaturation) for hematite (59%, 44 water sources) and negative values (undersaturation) for pyrite (71%, 53 water sources).

TDS and EC are directly related as reported elsewhere (e.g. Hem, 1985) (Fig. 7). Using the TDS-EC relationship, Dinelli et al. (2010) classified the Italian bottled mineral waters according to EC rather than

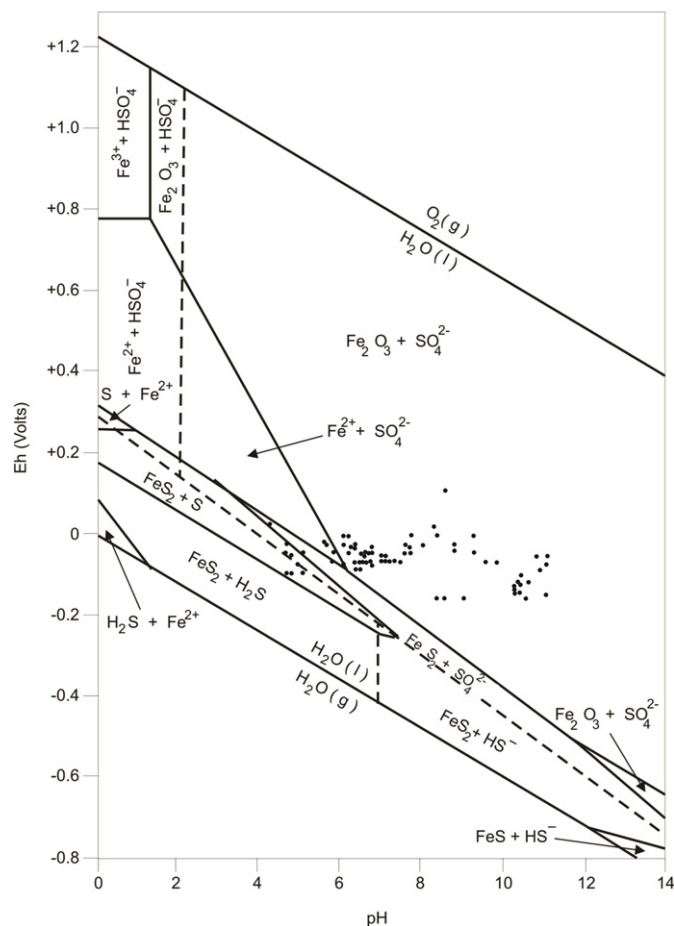


Fig. 6. Groundwater data plotted on Eh-pH diagram of iron oxides and sulfides in the presence of water at 25 °C temperature and 1 atm pressure, containing $\Sigma\text{S} = 0.1 \text{ M}$ (Faure, 1998). The dashed lines indicate the conditions under which the different S species become dominant.

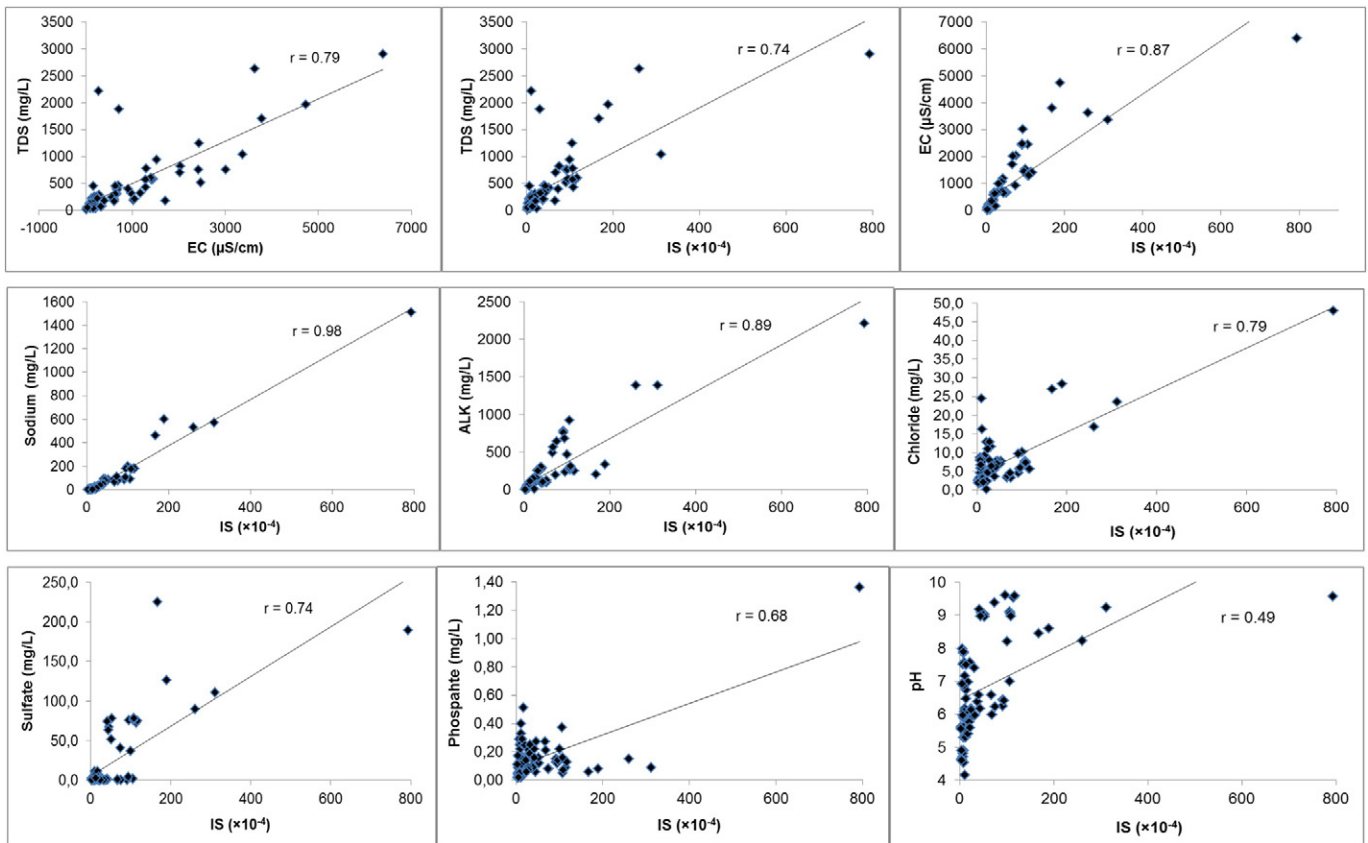


Fig. 7. The TDS-EC relationship and plots of the TDS, EC, sodium, total alkalinity (ALK), chloride, sulfate, phosphate and pH in the groundwater sources versus their ionic strength (IS).

TDS that is the parameter ruled by the EU mineral water directive (van der Aa, 2003). IS and TDS are also related ($r = 0.74$) (Fig. 7), implying on a IS-EC relationship (Fig. 7), despite the non-existence of a theoretical relation between them. The ions justifying such trends are sodium, (bi)-carbonate, chloride, sulfate and phosphate that are mathematically related with IS (Fig. 7) (Krauskopf and Bird, 1995). Sodium and sulfate correlated with pH, explaining the pH-IS relationship (Fig. 7).

The high SiO_2 concentration (Figs. 2 and 3) is a differential aspect of the spas groundwaters relative to many elsewhere. For instance, the analyses of 36 European mineral water brands reported by Eupedia (2016) show the following scenario for the molar ratios higher than unity: $\text{SiO}_2/\text{HCO}_3^-$ and $\text{SiO}_2/\text{Ca}^{2+} = 1$ mineral water (3%), $\text{SiO}_2/\text{Na}^+ = 2$ mineral waters (6%), $\text{SiO}_2/\text{Mg}^{2+} = 3$ mineral waters (8%), $\text{SiO}_2/\text{K}^+ = 11$ mineral waters (30%). This number is much higher in the spas groundwaters of this research (Tables 3 and 4): $\text{SiO}_2/\text{HCO}_3^- = 14$ water sources (19%), $\text{SiO}_2/\text{Na}^+ = 34$ water sources (45%), $\text{SiO}_2/\text{Ca}^{2+}$ and $\text{SiO}_2/\text{Mg}^{2+} = 75$ water sources (100%), $\text{SiO}_2/\text{K}^+ = 66$ water sources (88%).

Thus, several hydrochemical types represent the composition of waters from the different aquifer systems in this research. The great hydrochemical variability suggests that mixing of groundwaters from various sources often occur as recognized by Bonotto (2016) from the U-isotopes modeling. There is no way to obtain a consistent spatial representation of the hydrochemical facies in the whole study area. Very dilute waters suggesting the rainwater composition with small amounts of constituents added within the aquifers are widely spread. Additionally, saline waters also occur in some spas due to extensive chemical interaction between the groundwater and the aquifer materials.

5.3. Major sources influencing the groundwater composition

The aquifer systems investigated belong to two principal hydrogeological provinces: Paraná and Southeastern Shield (Mente,

2008). Such classification is general and does not allow discriminate between the shallower and deeper aquifers sometimes sampled in the same spa. This happened at Araxá, São Lourenço, Caxambu and Poços de Caldas spas (MG) where more superficial and deeper zones of water circulation could explain the main differences on the physico-chemical parameters (Cruz and Peixoto, 1989). Bertolo et al. (2007) pointed out that the groundwater flow in rapid and shallow (<70 m) systems would imply in waters with low mineralization, whereas the increase on the amount of dissolved species would tend to occur in deeper systems characterized by waters possessing long residence time. Additional aspects justifying such differences would certainly be the diverse lithology of the research area that comprises various types of magmatic, sedimentary and metamorphic rocks.

Aquachem 4.0 software (Waterloo Hydrogeologic, 2003) does the rock source deduction based on SiO_2 (in mmol/L), TDS (in mg/L), and the following ratios (Hounslow, 1995): $\text{HCO}_3^-/\text{SiO}_2$, $\text{SiO}_2/(\text{Na}^+ + \text{K}^+ - \text{Cl}^-)$, $(\text{Na}^+ + \text{K}^+ - \text{Cl}^-)/(\text{Na}^+ + \text{K}^+ - \text{Cl}^- + \text{Ca}^{2+})$, $\text{Na}^+/(\text{Na}^+ + \text{Cl}^-)$, $\text{Mg}^{2+}/(\text{Ca}^{2+} + \text{Mg}^{2+})$, $\text{Ca}^{2+}/(\text{Ca}^{2+} + \text{SO}_4^{2-})$, $\text{Cl}^-/\sum \text{anions}$, $\text{HCO}_3^-/\sum \text{anions}$. The aquifer systems in this research are inland, not suffering influence of processes affecting the coastal areas like salinisation due to sea water intrusion. Therefore, ratios evidencing them are not helpful for deducting some possible sources responsible by the presence of dissolved constituents in the liquid phase.

Demetriades (2010) have attributed Na^+/K^+ ratios <10 to rainwater, characterizing them in some bottled waters situated in areas with a comparatively high annual rainfall. In this paper, most of the waters analyzed (76%) exhibited Na^+/K^+ ratios <10 but many of them are not indicative of rapid groundwater flow as expected for a rainwater source. The $\text{Na}^+/(\text{Na}^+ + \text{Cl}^-)$ ratios <0.5 and TDS values <50 mg/L suggest a rainwater source according to the software Aquachem 4.0. They were found for the springs VIL (Águas da Prata – SP), COM (Águas de Lindóia – SP) and AMO (Pocinhos do Rio Verde – MG), agreeing with their location, flow conditions, and rainfall regime.

Demetriades (2010) found $(Ca^{2+} + Mg^{2+})/(Na^{+} + K^{+})$ ratios >1.0 in all bottled waters analyzed which would indicate that the aquifers are subjected to a continuous recharge. Equivalent ratios and processes have been identified from chemical and hydrogeological data of the samples coded BMU and AMO.

Demetriades (2010) evaluated $Cl^{-}/\sum anions <0.8$ in all bottled waters analyzed and pointed out that they could not be seriously affected by dissolution of halite or other evaporitic minerals. Equivalent ratios were also found in all spas groundwaters, yielding the “rock weathering” source classification by the Aquachem 4.0 software.

The rock source deduction by Aquachem 4.0 software based on the TDS concentration was “silicate weathering” (56 water sources, 75%) and “carbonate weathering” (19 water sources, 25%). The deduction from the HCO_3^{-}/SiO_2 ratio yielded “silicate weathering” (47 water sources, 63%), “carbonate weathering” (12 water sources, 16%) and mixed “silicate/carbonate weathering” source (16 water sources, 21%). These modeled rock sources are compatible with the respective lithologies of the sites.

Fluorite mineralization occurred in different stages of the hydrothermal event in PCAM (Holmes et al., 1992). Saturation indices for fluorite evaluated by the Aquachem 4.0 software indicated oversaturation in the springs RIV, SMA and SJO (Pocinhos do Rio Verde spa) and undersaturation in other groundwater samples. Anthropogenic inputs like the partially treated and untreated sewage, runoff from agricultural sites, and application of some lawn fertilizers cannot justify the dissolved PO_4^{3-} concentration in the spas groundwaters. Apatite occurs in PCAM and other geological contexts (Schorscher and Shea, 1992;

Traversa et al., 2001) and its dissolution may be the most probable PO_4^{3-} source in the water sources. It is a ubiquitous accessory mineral in igneous and metamorphic rocks whose solubility increases with temperature, pressure and raising of the NaCl mole fraction (Smith et al., 1977; Antignano and Manning, 2008). The highest phosphate concentration (1.36 mg/L) was in spring AJU at Araxá-MG spa, where a weathering mantle primarily enriched in P_2O_5 , Nb_2O_5 , TiO_2 , BaO and REE_2O_3 and resulting from the alteration of the alkaline-carbonatite rocks has been developed (Traversa et al., 2001). The weathering mantle also contains a large phosphate reserve situated at the northwestern portion of the carbonatitic complex (Traversa et al., 2001).

5.4. Geothermometry

The geothermometers use to both natural spring discharges and well fluids provides valuable insight to the nature of the system. Chemical geothermometers depend on the existence at depth of a mineral-fluid equilibrium temperature and its preservation during the fluid passage to the surface. Solute (water) geothermometers were empirically developed or based on thermodynamic properties. The most used are the silica (quartz and chalcedony), Na/K and Na–K–Ca geothermometers, also existing others based on Na/Li, Li/Mg, K/Mg ratios and Na–K–Mg relationships (Arnórsson, 2000). The choice of a specific geothermometer must take into account the temperature range for which it is valid as most of them only work above 100 °C (Arnórsson, 2000).

Geothermometers are generally derived from the Van't Hoff equation, allowing estimate the original subsurface reservoir temperature

Table 6

Geotemperatures (in °C) estimated according to the equations proposed by Fournier (1977) (SiO_2 geothermometer) and Arnórsson et al. (1983) (Na/K geothermometer).

Sample code	SiO_2 geotemperature	Na/K geotemperature	Sample code	SiO_2 geotemperature	Na/K geotemperature
ALS	91	278	LA6	52	975
GIO	47	3	SL7	86	603
JUV	71	−21	SL5	69	405
PLA	84	73	SL6	93	361
POL	78	69	SL3	90	311
VIT	83	82	SL4	65	576
BOI	61	2364	SL1	59	453
PTA	63	610	SL10	85	330
VIL	36	3704	SL9	66	448
PDE	62	695	ROR	61	556
SIL	57	594	REW	54	318
FIL	51	825	CAF	44	393
BEL	58	739	FEP	112	455
SRE	54	1259	MAR	111	615
COM	46	637	SLI	56	523
LIN	89	313	GFL	96	298
CUR	59	1444	VEN	90	308
SJO	60	288	MAY	65	981
SCA	85	457	EGU	106	310
ITA	85	446	VIO	69	915
SLU	72	275	DPE	66	619
SAT	78	296	BZA	111	300
BRU	83	315	DXE	94	334
LAN	64	254	LEO	95	251
SAA	86	410	ISA	113	368
SBE	92	425	QUI	39	608
BIO	64	947	NOV	77	149
JOR	85	8	MAC	81	143
ADB	83	3	SIN	82	138
CGO	85	4	FRA	27	502
SRC	84	−2	PEB	77	149
SEI	89	−3	RIV	80	135
BMU	91	408	SMA	77	144
LA1	44	766	SJO	78	148
LA2	47	728	AMO	42	2250
LA3	44	544	DBJ	69	2257
LA4	38	424	AJU	64	38
LA5	57	1116			

Table 7
Subsurface temperatures (in °C) estimated by the silica and Na/K geothermometers.

Sample code	Silica geothermometer		Na/K geothermometer	
	Ritter (2012)	This study	Ritter (2012)	This study
MAC	76–92	81	89–148	143
PEB	77–93	77	90–149	149
NOV	74–91	77	84–144	149

(T) of ascending groundwater which underwent conductive cooling during its ascent. The equation has the form (Waterloo Hydrogeologic, 2003):

$$T(\text{K}) = [a/(b + \log K)] + 273.15 \quad (2)$$

where: a and b are constants and K is the equilibrium constant that depends on the reaction used for the geothermometer.

The mineral-solution reaction using quartz (silica-geothermometer) is: $\text{SiO}_2(\text{qtz}) + 2\text{H}_2\text{O} = \text{H}_4\text{SiO}_4^0$. The cation exchange reaction between albite and K-feldspar depends on the temperature, supporting the Na/K geothermometer (Verma et al., 2008). Both feldspars are highly ordered with respect to Al and Si (low albite and microcline) and the reaction involved is (Arnórsson, 2000): $\text{NaAl}_3\text{Si}_3\text{O}_8 + \text{K}^+ = \text{KAl}_3\text{Si}_3\text{O}_8 + \text{Na}^+$.

The database in this research allowed estimate the silica and Na/K geotemperatures (Table 6) from the following equations (25 °C–250 °C) given by Fournier (1977) and Arnórsson et al. (1983), respectively:

$$T(\text{K}) = [1309/(5.19 - \log S)] - 273.15 \quad (3)$$

$$T(\text{K}) = [933/(0.993 + \log SP)] - 273.15 \quad (4)$$

where: S represents the dissolved SiO_2 concentration (in mg/L) and SP represents the Na/K ratio calculated from the dissolved Na and K contents (in mg/L).

Table 7 shows the geotemperatures for the springs MAC, PEB and NOV (Poços de Caldas-MG spa) estimated from Eqs. (3) and (4) and by Ritter (2012) from the SolGeo software (Verma et al., 2008). They practically agree for both geothermometers, inclusive in terms of the higher Na/K geotemperatures relative to the silica geotemperatures. Ritter (2012) pointed out that the missing quartz mineral phase in the host rock mineralogy of PCAM would make doubtful the application of the silica geothermometer there. However, most of the Na/K geotemperatures ranging from -21 °C (JUV spring) to 3704 °C (VIL spring) (Table 6) are impossible to occur in the aquifer systems investigated. Contrarily, the silica geotemperatures between 27 °C and 113 °C (Table 6) are possible in the old low-enthalpy and non-active volcanic systems investigated that differ of those described by Fournier (1977) and Arnórsson et al. (1983). In the case of PCAM, despite quartz is absent in the nepheline-syenites and phonolites, their SiO_2 concentration is 52.6%–55.6% (Schorscher and Shea, 1992). Thus, such SiO_2 levels favor its transfer into the liquid phase when the ascending waters interact with the aquifers rocks, justifying the silica geothermometer use.

6. Conclusion

Spas groundwaters from São Paulo (SP) and Minas Gerais (MG) states, Brazil, are an important resource extensively used for drinking in public places, bottling and bathing purposes, among others. This investigation involved the sampling 75 groundwaters from springs and tube wells occurring in 14 municipalities. The Brazilian Code of Mineral Waters (BCMW) guidelines indicated that most of them are cold (<25 °C), 44% are hypothermal (25–33 °C), one is mesothermal (33–36 °C), three are sulfured and one is ferruginous. The mineral waters EU directive allowed classify them as containing very low mineral concentration (TDS < 50 mg/L, 6 samples), low mineral concentration (TDS 50–

500 mg/L, 50 samples), intermediate mineral concentration (TDS 500–1500 mg/L, 13 samples), high mineral concentration (TDS > 1500 mg/L, 6 samples), bicarbonate ($\text{HCO}_3^- > 600$ mg/L – 7 samples), sulfate ($\text{SO}_4^{2-} > 200$ mg/L – 1 sample), fluoride ($\text{F}^- > 1$ mg/L – 24 samples), iron ($\text{Fe}^{2+} > 1$ mg/L – 3 samples), acidity ($\text{CO}_2 > 250$ mg/L – 36 samples), and sodium ($\text{Na}^+ > 200$ mg/L – 6 samples, 8%), whilst none exhibited chloride ($\text{Cl}^- > 200$ mg/L), calcium ($\text{Ca}^{2+} > 150$ mg/L) and magnesium ($\text{Mg}^{2+} > 50$ mg/L). Fluoride exceeded the WHO maximum allowable for ingestion in waters (1.5 mg/L) in 19 samples taken from two spas in SP and five spas in MG. The results of the data treatment and plotting according to Aquachem 4.0 software showed the occurrence of various hydrochemical facies, most of them dominated by the presence of HCO_3^- (CO_3^{2-}) and Na^+ . Additionally, silica was a significant constituent of all waters analyzed unlike most of European bottled mineral waters. The rock source deduction by Aquachem 4.0 software and based on Cl^-/\sum anions ratios < 0.8 in all water sources indicated the “rock weathering” source classification, whilst the TDS content (in mg/L) and $\text{HCO}_3^-/\text{SiO}_2$ ratios suggested the sources “silicate weathering”, “carbonate weathering” and mixed “silicate/carbonate weathering”. Testing the silica and Na/K geothermometers from the hydrochemical database allowed verify that most of the Na/K geotemperatures are impossible to occur in the natural systems, whereas the silica geotemperatures are compatible with the old low-enthalpy and non-active volcanic characteristics of the systems investigated.

Acknowledgments

The author thanks FAPESP (Foundation for Supporting Research at the State of São Paulo) (Proc. No. 2013/24360-6) and CNPq (National Council for Scientific and Technological Development) (Proc. No. 301462/2011-9), Brazil, for financial support of this investigation. Leila S. Marques and one anonymous reviewer are greatly thanked by helpful comments that improved the readability of the manuscript.

References

- Almeida, F.F.M., Hasui, Y., 1984. O Pré-cambriano do Brasil. Edgard Blücher, São Paulo (378 pp.).
- Alvarez, J.A., Rezende, K.M.P.C., Marocho, S.M.S., Alves, F.B.T., Celiberti, P., Ciamponi, A.L., 2009. Dental fluorosis: exposure, prevention and management. J. Clin. Exp. Dent. 1 (1), e14–e18.
- Antignano, A., Manning, C.E., 2008. Fluorapatite solubility in H_2O and $\text{H}_2\text{O-NaCl}$ at 700 to 900 °C and 0.7 to 2.0 GPa. Chem. Geol. 251, 112–119.
- APHA (American Public Health Association), 1989. Standard Methods for the Examination of Water and Wastewater. 17th ed. APHA, Washington, DC.
- Appelo, C.A.J., Postma, D., 2004. Geochemistry, Groundwater and Pollution. second ed. Balkema, New York.
- Arnórsson, S., 2000. Isotopic and Chemical Techniques in Geothermal Exploration, Development and Use: Sampling Methods, Data Handling, Interpretation. IAEA (International Atomic Energy Agency), Vienna (351 pp.).
- Arnórsson, S., Gunnlaugsson, E., Svavarsson, H., 1983. The chemistry of geothermal waters in Iceland. III. Chemical geothermometry in geothermal investigations. Geochim. Cosmochim. Acta 47, 567–577.
- Baas Becking, L.G.M., Kaplan, I.R., Moore, D., 1960. Limits of the natural environment in terms of pH and oxidation-reduction potential. J. Geol. 68, 243–284.
- Barnes, I., Back, W., 1964. Geochemistry of iron-rich groundwater of southern Maryland. J. Geol. 72, 435–447.
- Beato, D.A.C., Viana, H.S., Davis, E.G., 2000. Avaliação e diagnóstico hidrogeológico dos aquíferos de águas minerais do Barreiro do Araxá, MG, Brasil. Proc. I Joint World Congress on Groundwater, Fortaleza, pp. 1–20.
- Bertolo, R., Hirata, R., Fernandes, A., 2007. Hidrogeoquímica das águas minerais envasadas no Brasil. Rev. Bras. Geosci. 37, 2–15.
- Birke, M., Rauch, U., Lorenz, H., Kringsel, R., 2010a. Distribution of uranium in German bottled and tap water. J. Geochem. Explor. 107, 272–282.
- Birke, M., Rauch, U., Harazim, B., Lorenz, H., Glatte, W., 2010b. Major and trace elements in German bottled water, their regional distribution, and accordance with national and international standards. J. Geochem. Explor. 107, 245–271.
- Bitukova, L., Petersell, V., 2010. Chemical composition of bottled mineral waters in Estonia. J. Geochem. Explor. 107, 238–244.
- Bonotto, D.M., 2006. Hydro(radio)chemical relationships in the giant Guarani aquifer, Brazil. J. Hydrol. 323, 353–386.
- Bonotto, D.M., 2016. The dissolved uranium concentration and $^{234}\text{U}/^{238}\text{U}$ activity ratio in groundwaters from spas of southeastern Brazil. J. Environ. Radioact. <http://dx.doi.org/10.1016/j.jenvrad.2016.03.009>.

- Brenčič, M., Vreča, P., 2010. The use of a finite mixture distribution model in bottled water characterization and authentication with stable hydrogen, oxygen and carbon isotopes – case study from Slovenia. *J. Geochem. Explor.* 107, 391–399.
- Brenčič, M., Ferjan, T., Gosar, M., 2010. Geochemical survey of Slovenian bottled waters. *J. Geochem. Explor.* 107, 400–409.
- Brookins, D.G., 1988. Eh-pH Diagrams for Geochemistry. Springer-Verlag, Berlin (176 pp.).
- Brownlow, A.H., 1996. Geochemistry. second ed. Prentice-Hall, Englewood Cliffs (580 pp.).
- Cicchella, D., Albanese, S., De Vivo, B., Dinelli, E., Giaccio, L., Lima, A., Valera, P., 2010. Trace elements and ions in Italian bottled mineral waters: identification of anomalous values and human health related effects. *J. Geochem. Explor.* 107, 336–349.
- CPRM (Brazilian Geological Survey), 1999. Projeto Circuito das Águas do Estado de Minas Gerais – Estudos Geoambientais das Fontes Hidrominerais de Águas de Contendas, Cambuquira, Caxambu, Lambari e São Lourenço. CPRM, Belo Horizonte (142 pp.).
- CPRM (Brazilian Geological Survey), 2008. Geologia da Folha Varginha SF.23-V-D-VI. CPRM, Brasília (99 pp.).
- CPRM (Brazilian Geological Survey), 2012. A indústria brasileira de água mineral. <http://www.cprm.gov.br/>.
- Cruz, W.B., Peixoto, C.A.M., 1989. Águas termais de Poços de Caldas, MG: estudo experimental das interações água-rocha. *Rev. Bras. Geosci.* 19, 76–86.
- Custodio, E.G., Llamas, M.R., 1976. Hidrologia Subterránea (T. 1). first ed. Omega, Barcelona.
- Davenward, S., Bentham, P., Wright, J., Crome, P., Job, D., Polwart, A., Exley, C., 2013. Silicon-rich mineral water as a non-invasive test of the 'aluminum hypothesis' in Alzheimer's disease. *J. Alzheimers Dis.* 33 (2), 423–430.
- del Rey, A.C., 1989. Estudo hidrogeotérmico da região de Águas de Lindóia, Amparo e Sororro-nordeste do Estado de São Paulo (Ms Dissertation) USP-University of São Paulo, São Paulo (124 pp.).
- Demetriades, A., 2010. General ground water geochemistry of Hellas using bottled water samples. *J. Geochem. Explor.* 107, 283–298.
- DPPM (Division for Supporting the Mineral Production), 1966. The Mining Code, the Mineral Waters Code and how Applying Research in a Mineral Deposit. eighth ed. DPPM, Rio de Janeiro.
- Dinelli, E., Lima, A., De Vivo, B., Albanese, S., Cicchella, D., Valera, P., 2010. Hydrogeochemical analysis of Italian bottled mineral waters: effects of geology. *J. Geochem. Explor.* 107, 317–335.
- Dotsika, E., Poutoukis, D., Raco, B., Psomiadis, D., 2010. Stable isotope composition of Hellenic bottled waters. *J. Geochem. Explor.* 107, 299–304.
- Dušan, B., Jozef, K., Igor, S., Peter, M., Pavel, L., Daniel, P., Jarmila, B., Daniel, M., 2010. Mineral waters in Slovakia – evaluation of chemical composition stability using both historical records and the most recent data. *J. Geochem. Explor.* 107, 382–390.
- Ebert, H., 1955. Sedimentos metamórficos de origem clástica e sua significação para o esclarecimento da estrutura geológica do Escudo Cristalino Brasileiro. *Engenharia Mineração Metal.* 22, 39–40.
- Edmunds, W.M., Smedley, P.L., 2013. Fluoride in natural waters. In: Selinus, O., Alloway, B., Centeno, J.A., Finkelman, R.B., Fuge, R., Lindh, U., Smedley, P.L. (Eds.), *Essentials of Medical Geology*. Springer, Heidelberg, pp. 311–336.
- Ellert, R., 1959. Contribuição à geologia do maciço alcalino de Poços de Caldas. *Bol. Geol. FFCL USP* 237, 5–64.
- Eupedia, 2016. Mineral analysis of a few European mineral water brands. http://www.eupedia.com/europe/european_mineral_waters.shtml.
- Faure, G., 1998. Principles and Applications of Geochemistry. second ed. Prentice-Hall, Upper Saddle River, NJ (600 pp.).
- Fournier, R.O., 1977. Chemical geothermometers and mixing models for geothermal systems. *Geothermics* 5, 41–50.
- Frengstad, B.S., Lax, K., Tarvainen, T., Jæger, Ø., Wigum, B.J., 2010. The chemistry of bottled mineral and spring waters from Norway, Sweden, Finland and Iceland. *J. Geochem. Explor.* 107, 350–361.
- Fugedi, U., Kuti, L., Jordan, G., Kerek, B., 2010. Investigation of the hydrogeochemistry of some bottled mineral waters in Hungary. *J. Geochem. Explor.* 107, 305–316.
- Garrels, R.M., 1959. *Mineral Equilibria*. Addison-Wesley Reading, Mass. (349 pp.).
- Garrels, R.M., Christ, C.L., 1965. *Minerals, Solutions and Equilibria*. Harper & Row, New York (453 pp.).
- Gibson, S.A., Thompson, R.N., Dickin, A.P., Leonardos, O.H., 1995a. High-Ti and low-Ti mafic potassic magmas: key to plume-lithosphere interactions and continental flood basalt genesis. *Earth Planet. Sci. Lett.* 136, 149–165.
- Gibson, S.A., Thompson, R.N., Leonardos, O.K., Dickin, A.P., Mitchell, J.G., 1995b. The Late Cretaceous impact of the Trindade mantle plume - evidence from large-volume, mafic, potassic magmatism in SE Brazil. *J. Petrol.* 36, 189–229.
- Godoy, J.M., Amaral, E.C.S., Godoy, M.L.D.P., 2001. Natural radionuclides in Brazilian mineral water and consequent doses to the population. *J. Environ. Radioact.* 53, 175–182.
- Gomes, C.B., Comin-Chiaramonti, P., 2005. Some notes on the Alto Paranaíba igneous province. In: Comin-Chiaramonti, P., Gomes, C.B. (Eds.), *Mesozoic to Cenozoic Alkaline Magmatism in the Brazilian Platform*. EDUSP, São Paulo, pp. 317–340.
- Hach, 1992. *Water Analysis Handbook*. second ed. Hach Co., Loveland (831 pp.).
- Hem, J.D., 1985. Study and interpretation of the chemical characteristics of natural waters. U.S. Geological Survey, Water-Supply Paper 2254, third ed.
- Holmes, D., C., Pitty, A.E., Noy, D.J., 1992. Geomorphological and hydrogeological features of the Poços de Caldas caldera analogue study sites. *J. Geochem. Explor.* 45, 215–247.
- Hounslow, A.W., 1995. *Water Quality Data – Analysis and Interpretation*. Lewis Publishers, Boca Raton (397 pp.).
- Hydrogeologic, W., 2003. *AquaChem User's Manual: Water Quality Data Analysis, Plotting & Modeling*. Waterloo Hydrogeologic, Waterloo (276 pp.).
- IPT (Technological Research Institute of São Paulo State), 1981. Geological Map From São Paulo State: Scale 1:500.000. Monographs. IPT, São Paulo (94 pp.).
- Kimmelman, A.A., Yoshinaga, S., Murakami, H., Mattos, J.A., 1987. Novos aspectos hidrogeológicos, hidroquímicos e isotópicos das águas termominerais de Águas de São Pedro no Estado de São Paulo. *Proc. VII Simp. Bras. de Hidrologia e Rec. Hídricos*, Salvador, pp. 26–41.
- Krauskopf, K.B., Bird, D.K., 1995. *Introduction to Geochemistry*. McGraw-Hill Inc., New York (647 pp.).
- Lourenço, C., Ribeiro, L., Cruz, J., 2010. Classification of natural mineral and spring bottled waters of Portugal using principal component analysis. *J. Geochem. Explor.* 107, 362–372.
- Mente, A., 2008. Mapa Hidrogeológico do Brasil. In: Feitosa, F.A.C., Manoel Filho, J., Feitosa, E.C., Demetrio, J.G. (Eds.), *Hidrogeologia - conceitos e aplicações*. CPRM-LABHID, Rio de Janeiro, pp. 31–48.
- Milani, E.J., 2004. Comentários sobre a origem e evolução tectônica da Bacia do Paraná. In: Mantesso-Neto, V., Bartorelli, A., Carneiro, C.D.R., Brito-Neves, B.B. (Eds.), *Geologia do Continente Sul-Americano: Evolução da Obra de Fernando Flávio de Almeida*. Beca, São Paulo, pp. 265–279.
- Mourão, B.M., 1992. *Medicina hidrológica - Moderna terapêutica das águas minerais e estâncias de cura*. Secretaria Municipal de Educação, Poços de Caldas.
- Oliveira, J., Mazzilli, B.P., Sampa, M.H.O., Silva, B., 1998. Seasonal variations of Ra-226 and Rn-222 in mineral spring waters of Águas da Prata-Brazil. *Appl. Radiat. Isot.* 49 (4), 423–427.
- Oliveira, J., Mazzilli, B., Costa, P., Tanigawa, P.A., 2001. Natural radioactivity in Brazilian bottled mineral waters and consequent doses. *J. Radioanal. Nucl. Chem.* 249 (1), 173–176.
- Peh, Z., Šorša, A., Halamić, J., 2010. Composition and variation of major and trace elements in Croatian bottled waters. *J. Geochem. Explor.* 107, 227–237.
- Petrović, T., Zlokolica-Mandić, M., Veljković, N., Vidojević, D., 2010. Hydrogeological conditions for the forming and quality of mineral waters in Serbia. *J. Geochem. Explor.* 107, 373–381.
- Piper, A.M., 1944. A graphic procedure in the geochemical interpretation of water analyses. *Trans. Am. Geophys. Union* 25, 914–928.
- Reddy, D.V., Nagabhushanam, P., Sukhija, B.S., Reddy, A.G.S., Smedley, P., 2010. Fluoride dynamics in the granitic aquifer of the Wailapally watershed, Nalgonda District, India. *Chem. Geol.* 269, 278–289.
- Renne, P.R., Ernesto, M., Pacca, I.G., Coe, R.S., Glen, J.M., Prévot, M., Perrin, M., 1992. The age of Paraná flood volcanism, rifting of Gondwanaland, and the Jurassic-Cretaceous boundary. *Science* 258, 975–979.
- Ritter, S.M., 2012. *Geothermometry on Natural Spring Waters From Poços de Caldas, Minas Gerais, Brazil*. Monograph. University of Heidelberg, Heidelberg (56 pp.).
- Schoeller, H., 1962. *Les eaux souterraines*. Masson & Cie, Paris (642 pp.).
- Schorscher, J.H.D., Shea, M.E., 1992. The regional geology of the Poços de Caldas alkaline complex: mineralogy and geochemistry of selected nepheline syenites and phonolites. *J. Geochem. Explor.* 45, 25–51.
- SEBRAE (Service for Supporting the Small Businesses in São Paulo State), 2012o. Comércio de água mineral. <http://www.sebrae-sc.com.br/ideias/default.asp?vcdtexto=315868%5E%5E>.
- Serra, S.H., 2009. *Águas minerais do Brasil*. Millenium Editora, Campinas (272 pp.).
- Smedley, P.L., Nicolli, H.B., Macdonald, D.M.J., Barros, A.J., Tullio, J.O., 2002. Hydrogeochemistry of arsenic and other inorganic constituents in groundwaters from La Pampa, Argentina. *Appl. Geochem.* 17, 259–284.
- Smith, E.A., Mayfield, C.I., Wong, P.T.S., 1977. Physical and chemical characterization of selected natural apatites in synthetic and natural aqueous solutions. *Water Air Soil Pollut.* 8, 401–415.
- Szikszy, M., 1981. Hidrogeoquímica das fontes de Águas da Prata, Estado de São Paulo (Post PhD Thesis) USP-University of São Paulo, São Paulo (193 pp.).
- Thiede, D.S., Vasconcelos, P.M., 2010. Paraná flood basalts: rapid extrusion hypothesis confirmed by new ⁴⁰Ar/³⁹Ar results. *Geology* 38 (8), 747–750.
- Thompson, R.N., Gibson, S.A., Mitchell, J.G., Dickin, A.P., Leonardos, O.K., Brod, J.A., Greenwood, J.C., 1998. Migrating Cretaceous-Eocene magmatism in the Serra do Mar alkaline province, SE Brazil: melts from the deflected Trindade mantle plume? *J. Petrol.* 39, 1493–1526.
- Traversa, G., Gomes, C.B., Brotzu, P., Buraglini, N., Morbidelli, L., Principato, M.S., Ronca, S., Ruberti, E., 2001. Petrography and mineral chemistry of carbonates and mica-rich rocks from the Araxá complex (Alto Paranaíba Province, Brazil). *Am. Acad. Bras. Cienc.* 73, 71–98.
- Turner, S., Regelous, M., Kelley, S., Hawkesworth, C.J., Mantovani, M.S.M., 1994. Magmatism and continental break-up in the South Atlantic: high precision ⁴⁰Ar-³⁹Ar geochronology. *Earth Planet. Sci. Lett.* 121, 333–348.
- Ulbrich, H.H.G.J., Vlach, S.R.F., Demaiffe, D., Ulbrich, M.N.C., 2005. Structure and origin of the Poços de Caldas alkaline massif. In: Comin-Chiaramonti, P., Gomes, C.B. (Eds.), *Mesozoic to Cenozoic Alkaline Magmatism in the Brazilian Platform*. EDUSP, São Paulo, pp. 367–418.
- Van der Aa, M., 2003. Classification of mineral water types and comparison with drinking water standards. *Environ. Geol.* 44, 554–563.
- Verma, S.P., Pandarinath, K., Santoyo, E., 2008. SolGeo: a new computer program for solute geothermometers and its application to Mexican geothermal fields. *Geothermics* 37, 597–621.
- WHO (World Health Organization), 2011. *Guidelines for Drinking Water Quality*. fourth ed. WHO Press, Geneva.
- Zanardo, A., 1987. Análise petrográfica e microestrutural das rochas da Folha de Águas de Lindóia. USP-University of São Paulo, São Paulo, Ms Dissertation (270 pp.).
- Zobell, C.E., 1946. Studies on redox potential of marine sediments. *Bull. Am. Assoc. Pet. Geol.* 30, 477–509.